Original Research Article

Cervical Spinal Cord Atrophy can be Accurately Quantified Using Head Images

Kamyar Taheri, BSc (iD), Irene M Vavasour, PhD (iD), Shawna Abel, MSc (iD), Lisa Eunyoung Lee, MSc (iD), Poljanka Johnson, BSc, Stephen Ristow, BSc, Roger Tam, PhD, Cornelia Laule, Phd, Nathalie Chantal Ackermans, MD (iD), Alice Schabas, MD, Helen Cross, MD, Jillian Katrina Chan, MD, Ana-Luiza Sayao, MD, Virender Bhan, MD, Virginia Devonshire, MD, Robert Carruthers, MD (iD), David KB Li, MD, Anthony L Traboulsee, MD, Shannon H Kolind, PhD* and Adam Vladimir Dvorak, BSc* (iD)

Abstract

Background: Spinal cord atrophy provides a clinically relevant metric for monitoring MS. However, the spinal cord is imaged far less frequently than brain due to artefacts and acquisition time, whereas MRI of the brain is routinely performed.

Objective: To validate spinal cord cross-sectional area measurements from routine 3DT1 whole-brain MRI versus those from dedicated cord MRI in healthy controls and people with MS.

Methods: We calculated cross-sectional area at C1 and C2/3 using T2*-weighted spinal cord images and 3DT1 brain images, for 28 healthy controls and 73 people with MS. Correlations for both groups were assessed between: (1) C1 and C2/3 using cord images; (2) C1 from brain and C1 from cord; and (3) C1 from brain and C2/3 from cord.

Results and Conclusion: C1 and C2/3 from cord were strongly correlated in controls ($r = 0.94$, $p<0.0001$) and MS ($r = 0.85$, $p<0.0001$). There was strong agreement between C1 from brain and C2/3 from cord in controls ($r = 0.84$, $p<0.0001$) and MS ($r = 0.81$, $p<0.0001$). This supports the use of C1 cross-sectional area calculated from brain imaging as a surrogate for the traditional C2/3 cross-sectional area measure for spinal cord atrophy.

Keywords: Spinal cord, magnetic resonance imaging, multiple sclerosis, atrophy, neuroimaging, cervical cord

Introduction

Multiple Sclerosis (MS) is an inflammatory, demyelinating disease that causes neurodegeneration in the central nervous system. Cord atrophy measurements from magnetic resonance imaging (MRI)[1] provide a valuable and clinically relevant metric for monitoring MS.[2] The C2/3 segment of the cervical cord is often used to assess atrophy in MS due to its high concentration of lesions, increased rate of atrophy, and relative technical ease compared to assessment of the whole cord.[3–5]

Spinal cord is imaged far less frequently than brain due to artefacts and acquisition time.[1,6] 3-dimensional, T1-weighted (3DT1) brain images, which are recommended for volumetric assessment of MS brain,[7] often capture a few upper cervical spinal cord levels, depending on the field-of-view (FOV). If C1 cross-sectional area (CSA) accurately reflects C2/3 CSA, which has been established as clinically relevant, and CSA measurements derived from brain images agree with spinal cord image values, then a clinically relevant measure of spinal cord atrophy could be obtained using only a standard 3DT1 brain image. Previously, Liu et al. showed strong agreement between upper cervical cord area values calculated from 3D T1-weighted images of the head and cord.[8] In 2018, Papinutto et al. demonstrated that reproducible upper cervical cord area measurements can be derived from head images, so

Correspondence to:
Dr Shannon H Kolind,
University of British Columbia, S199-2211 Wesbrook Mall, Vancouver BC, Canada, V6 T 2B5.
shannon.kolind@ubc.ca

*Shared Senior Author

Kamyar Taheri,
Department of Medicine, University of British Columbia, Vancouver, BC, Canada

Irene M Vavasour,
Department of Radiology, University of British Columbia, Vancouver, BC, Canada

Shawna Abel,
Lisa Eunyoung Lee,
Poljanka Johnson,
Stephen Ristow,
Department of Medicine, University of British Columbia, Vancouver, BC, Canada

Roger Tam,
Department of Radiology, University of British Columbia, Vancouver, BC, Canada

Cornelia Laule,
Department of Radiology, University of British Columbia, Vancouver, BC, Canada
Department of Pathology & Laboratory Medicine, University of British Columbia, Vancouver, BC, Canada
Department of Physics & Astronomy, University of British Columbia, Vancouver, BC, Canada
International Collaboration on Repair Discoveries (ICORD), Vancouver, BC, Canada

Nathalie
Chantal Ackermans,
Alice Schabas,
Helen Cross,
Jillian Katrina Chan,
Ana-Luiza Sayao,
Virender Bhan,
Virginia Devonshire,
Robert Carruthers,
Department of Medicine, University of British Columbia, Vancouver, BC, Canada

David KB Li,
Department of Medicine, University of British Columbia, Vancouver, BC, Canada
Department of Radiology, University of British Columbia, Vancouver, BC, Canada

Anthony L Traboulsee,
Department of Medicine, University of British Columbia, Vancouver, BC, Canada

Shannon H Kolind,
Department of Medicine, University of British Columbia, Vancouver, BC, Canada
Department of Radiology, University of British Columbia, Vancouver, BC, Canada
Department of Physics & Astronomy, University of British Columbia, Vancouver, BC, Canada
International Collaboration on Repair Discoveries (ICORD), Vancouver, BC, Canada

long as corrections for gradient non-linearities are performed.[9]

The overall aim of this study was to determine if measurements of C1 CSA, derived from 3DT1 brain images, can provide a surrogate measurement for C2/3 CSA measurements obtained from dedicated spinal cord imaging. All groupwise analyses were performed for both healthy controls and people with MS. We first investigated the relationship between C1 CSA calculated from cord images versus C2/3 CSA calculated from cord images. We then assessed the agreement between C1 CSA calculated from brain images and C1 CSA calculated from cord images. Finally, we directly assessed the relationship between C1 CSA calculated from brain images (our proposed cord atrophy surrogate measure) and C2/3 CSA calculated from spinal cord images. This work builds upon previous literature by 1) directly comparing values from standard 3DT1 brain imaging to those from multi-gradient echo T2*-weighted cord imaging, recommended by the International Spinal Cord Society (ISCoS)[10] and 2) maximizing applicability by using only default vendor-implemented gradient non-linearity corrections and processing with Spinal Cord Toolbox (SCT),[11,12] the standard for cord atrophy analysis.

Materials and methods

Participants

The study was approved by the University of British Columbia Clinical Research Ethics Board. All participants provided written informed consent prior to participation. We collected data from 28 healthy controls (11 M/17 F, mean age 47 years, age range 22–65 years) and 73 people with clinically definite MS, fulfilling the 2017 revised McDonald criteria for diagnosis,[13] (25 M/48 F, mean age 50 years, age range 26–65 years, 38 relapsing-remitting MS (RRMS); 12 primary progressive MS (PPMS); 23 secondary progressive MS (SPMS), median Expanded Disability Status Scale (EDSS)[14] 3.5, EDSS range 1.0–8.5, median disease duration 12.0 years, disease duration range 0.3–48 years). Control and MS groups did not differ significantly in age or sex ($p > 0.10$). De-identified data will be shared following a reasonable request by a qualified investigator.

Imaging

Data was collected at the UBC MRI Research Centre on a 3.0 Tesla MRI scanner (Achieva, Philips Healthcare, Best, The Netherlands). For brain imaging, a 3D T1-weighted magnetization-prepared rapid gradient-echo sequence was acquired (resolution $1 \times 1 \times 1$ mm, FOV = $256 \times 256 \times 165$ mm, repetition time (TR) = 8.1 ms, echo time (TE) = 2.5 ms, inversion time (TI) = 1052 ms, shot interval = 3000 ms, acquisition time = 6 min 26 s) using an 8-channel head coil. For spinal cord imaging, a T2*-weighted multi-echo rapid gradient echo scan was collected (resolution $0.8 \times 0.8 \times 2.5$ mm, FOV = $150 \times 150 \times 44$ mm, TR = 815 ms, TE = 6.5 ms, ΔTE = 8.2 ms, 5 echoes (cumulated on the scanner), acquisition time = 5 min 7 s) using a 6-channel spine coil with the FOV centred at the level of the C2/3 disc. Brain and spinal cord data was collected during the same scan session. All images were reconstructed including the default vendor-implemented gradient non-linearity corrections.

Analysis

SCT[11,12] was used to (1) automatically segment the spinal cord[15], (2) label cord vertebral levels using the manually identified C2/3 disc and image intensity of the vertebral columns and intervertebral discs, and (3) extract the mean cord CSA using the SCT segmentation across all image slices contained in the C1 level and in the C2/3 levels. CSA derived from brain images is abbreviated as CSA_{brain} and CSA derived from spinal cord images is abbreviated as CSA_{cord}. Manual quality control was performed to ensure accuracy of the cord segmentation and labelling of the cord vertebral levels.

All statistical analyses were performed for both control and MS groups. We compared: **(1) C1 CSA_{cord} versus C2/3 CSA_{cord}**, to check for underlying correspondence between CSA at these different anatomical locations, **(2) C1 CSA_{brain} versus C1 CSA_{cord}**, to assess the agreement between CSA calculated for the same location from standard brain 3DT1 images and from ISCoS recommended T2*-weighted cord images, and **(3) C1 CSA_{brain} versus C2/3 CSA_{cord}**, to provide a direct validation of the ability to use C1 CSA_{brain} as a surrogate for C2/3 CSA_{cord}. For all comparisons, Spearman correlation coefficients (r) and 95% confidence intervals were calculated for relationships between CSA_{cord} or CSA_{brain} at different levels. Linear regression was used to model the relationships between CSA measures. Finally, Bland-Altman analysis was used to assess their agreement accounting for bias. For C1 CSA_{brain} versus C1 CSA_{cord}, the only comparison between paired values of the same measure, Wilcoxon paired t-tests were used to assess the agreement between CSA_{brain} and CSA_{cord}, presented as means with 95% confidence intervals. We chose to use non-
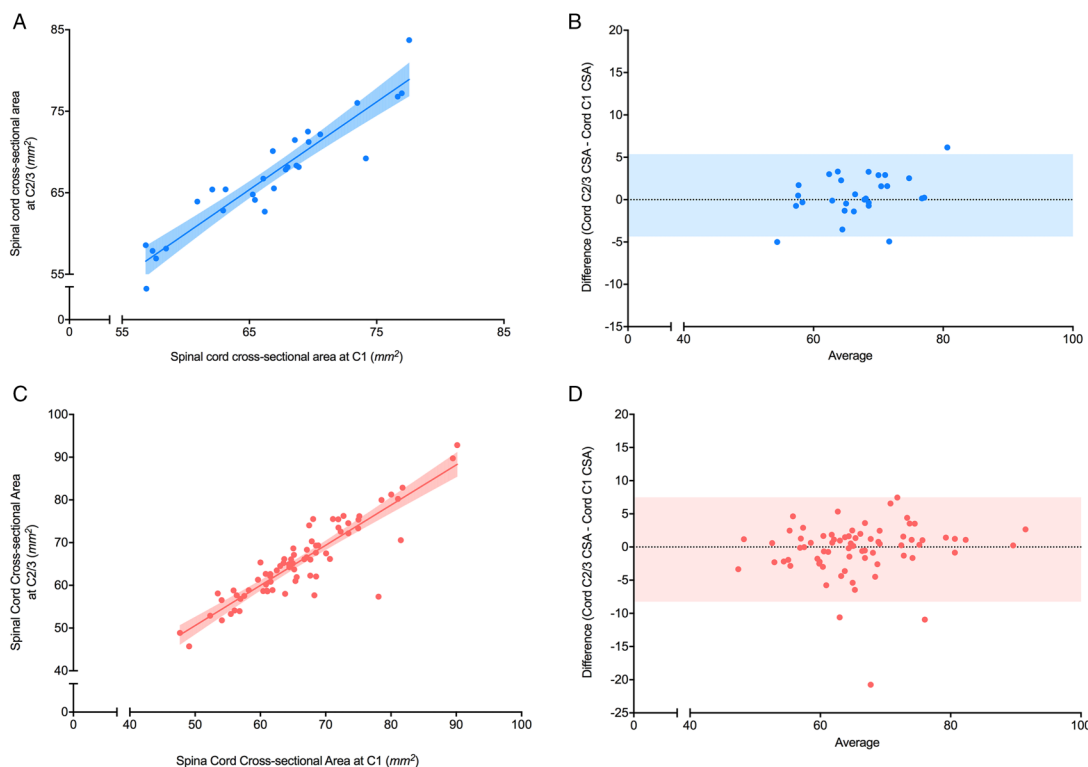
Adam Vladimir Dvorak,
Department of Physics &
Astronomy, University of
British Columbia,
Vancouver, BC, Canada
International Collaboration
on Repair Discoveries
(ICORD), Vancouver, BC,
Canada

Figure 1. Correlation between C1 CSA with C2/3 CSA from cord imaging in healthy controls and people with multiple sclerosis (MS). (A) Correlation between spinal cord cross-sectional area (CSA) (mm^2) from healthy controls measured using spinal cord imaging at C1 and at C2/3 ($n = 28$). The r value was 0.94 with $p<0.0001$. A linear regression model was used to fit the data with r^2 value of 0.88, slope of 1.1, and y-intercept of -4.6 mm^2. The shaded areas represent the 95% confidence intervals. (B) Bland-Altman plot between spinal cord CSA (mm^2) from healthy controls measured using cord imaging at C1 and at C2/3. A bias of 0.50 mm^2 and 95% limits of agreement (shaded region) from -4.4 to 5.4 mm^2 were found. (C) Correlation between spinal cord CSA (mm^2) measured from people with MS measured at C1 and at C2/3 using cord imaging ($n = 73$). The r value was 0.85 with $p<0.0001$. A linear regression model was used to fit the data with $r^2 = 0.80$, slope $= 0.94$, and y-intercept $= 3.6$ mm^2. The shaded area represents the 95% confidence interval. (D) Bland-Altman plot for spinal cord CSA (mm^2) measured from people with MS at C1 and at C2/3 using cord images. A bias of -0.38 mm^2 and a 95% limit (shaded region) of agreement from -8.2 to 7.5 mm^2 was found.

parametric analyses due to our sample size, especially for the healthy control group with fewer than 30 subjects, because 30 is the minimum number suggested for analyses assuming a parametric distribution. All statistical analysis was done using GraphPad Prism 7.

Results

C1 CSA$_{cord}$ versus C2/3 CSA$_{cord}$

Controls. C1 CSA$_{cord}$ was positively correlated with C2/3 CSA$_{cord}$ in the control group ($r = 0.94$ (0.89–0.97), $p<0.0001$, Figure 1A) with a linear regression model slope of 1.1 and y-intercept of -4.6 mm^2 ($r^2 = 0.88$). Bland-Altman analysis showed a bias of 0.50 mm^2, a 95% limit of agreement of -4.4 to 5.4 mm^2, and no significant non-zero slope ($p = 0.052$; Figure 1B).

Multiple sclerosis. C1 CSA$_{cord}$ was positively correlated with C2/C3 CSA$_{cord}$ in people with MS ($r = 0.85$ (0.77–0.91), $p<0.0001$, Figure 1C) with a linear regression model slope of 0.94 and y-intercept of 3.6 mm^2 (r^2 of 0.80). Bland-Altman analysis showed a bias of -0.38 mm^2, a 95% limit of agreement of -8.2 to 7.5 mm^2 and no significant non-zero slope ($p = 0.37$; Figure 1D).

C1 CSA$_{brain}$ versus C1 CSA$_{cord}$

Controls. The relationship between C1 CSA$_{cord}$ and C1 CSA$_{brain}$ showed a positive correlation ($r = 0.89$ (0.78–0.95), $p<0.0001$, Figure 2A) with a linear regression model slope of 0.74 and a y-intercept 16 mm^2 ($r^2 = 0.73$). Bland-Altman analysis showed a bias of 2.4 mm^2, a 95% limit of agreement of -4.7 to 9.6 mm^2 and no significant non-zero slope ($p =$
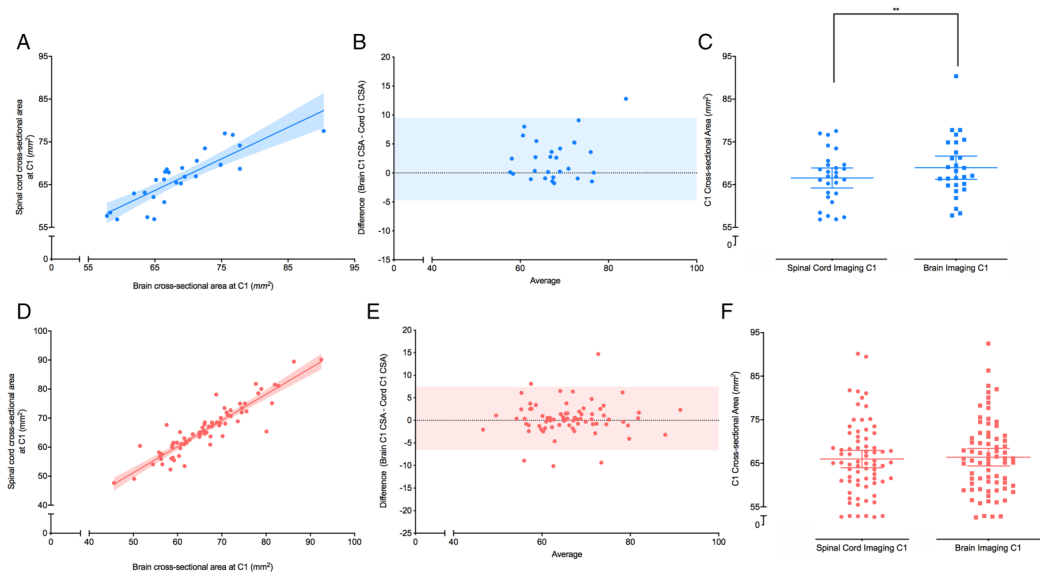
Figure 2. Correlation between C1 CSA from brain imaging with C1 CSA from cord imaging in healthy controls and people with multiple sclerosis (MS). (A) Correlation between spinal cord cross-sectional area (CSA) (mm^2) from healthy controls measured at C1 using T1-weighted brain imaging and T2*-weighted cord imaging. The r value was 0.89 with $p<0.0001$. A linear regression model was used to fit the data with r^2 value of 0.73, slope of 0.74, and y-intercept of 16 mm^2. The shaded area represents the 95% confidence interval ($n = 28$). (B) Bland-Altman plot between spinal cord CSA (mm^2) from healthy controls measured at C1 using brain imaging and cord imaging. A bias of 2.4 mm^2 and 95% limits of agreement (shaded region) from −4.7 to 9.6 mm^2 were found. (C) Grouped analysis of spinal cord CSA (mm^2) from healthy controls measured at C1 using cord (circles) and brain (squares) imaging. The spinal cord CSA had a mean of 66 (64–69) mm^2 and the brain C1 CSA had a mean of 69 (66–72) mm^2. Mean and 95% confidence intervals of each group are shown. A non-parametric Wilcoxon paired t-test showed a significant mean difference of 2.4 (1.0–3.8) mm^2 with $p = 0.0041$. (D) Correlation between C1 CSA (mm^2) from people with MS measured using T1-weighted brain imaging and T2*-weighted cord imaging. The r value was 0.91 with $p<0.0001$. A linear regression model was used to fit the data with r^2 value of 0.83, slope of 0.90, and y-intercept of 6.2 mm^2. The shaded area represents the 95% confidence interval ($n = 73$). (E) Bland-Altman plot between C1 CSA (mm^2) from people with MS measured using brain imaging and cord imaging. A bias of 0.43 mm^2 and 95% limits of agreement (shaded region) from −6.6 to 7.5 mm^2 were found ($n = 73$). (F) Grouped analysis of spinal cord CSA (mm^2) from people with MS measured at C1 using cord (circles) and brain (squares) imaging. The spinal cord CSA had a mean of 66 (64–68) mm^2 and the brain C1 CSA had a mean of 66 (64–68) mm^2. Mean and 95% confidence intervals of each group are shown. A non-parametric Wilcoxon paired t-test for the mean difference of 0.4 mm^2 was not significant with $p > 0.2$.

0.16, Figure 2B). A non-parametric t-test showed a small but significant difference of 2.4 mm^2 (1.0–3.8 mm^2, $p = 0.0041$) between C1 CSA$_{cord}$ (mean = 66 mm^2, 64–69 mm^2 95% CI) and C1 CSA$_{brain}$ (mean = 69 mm^2, 66–72 mm^2 95% CI) in the control group (Figure 2C).
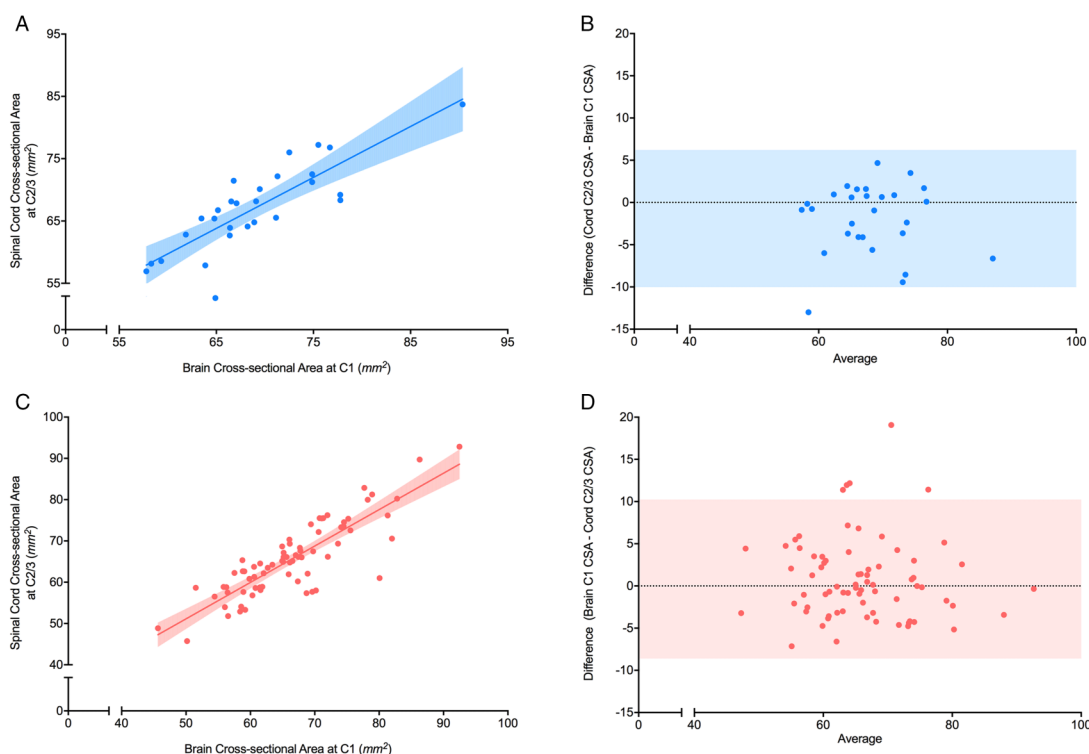
Multiple sclerosis. The relationship between C1 CSA$_{cord}$ to C1 CSA$_{brain}$ for MS also showed a positive correlation ($r = 0.91$ (0.86–0.94), $p<0.0001$, Figure 2D) with a linear regression model slope of 0.90 and a y-intercept of 6.2 mm^2 ($r^2 = 0.83$). Bland-Altman analysis showed a bias of 0.43 mm^2, a 95% limit of agreement of −6.6 to 7.5 mm^2, and no significant non-zero slope ($p = 0.78$, Figure 2E). A non-parametric t-test for the mean difference of 0.4 mm^2 was not significant ($p > 0.2$) between C1 CSA$_{cord}$ (mean = 66 mm^2, 64–68 mm^2 95% CI) and

C1 CSA$_{brain}$ (mean = 66 mm^2, 64–68 mm^2 95% CI) in people with MS (Figure 2F).

C1 CSA$_{brain}$ versus C2/3 CSA$_{cord}$

Controls. C1 CSA$_{brain}$ was positively correlated with C2/3 CSA$_{cord}$ in healthy individuals ($r = 0.84$ (0.68–0.92), $p<0.0001$, Figure 3A) with a linear regression model slope of 0.82 and y-intercept 11 mm^2 ($r^2 = 0.68$). Bland-Altman analysis showed a bias of −1.9 mm^2, a 95% limit of agreement of −10 to 6.2 mm^2 and no significant non-zero slope ($p = 0.095$, Figure 3B).

Multiple sclerosis. C1 CSA$_{brain}$ was also positively correlated with C2/3 CSA$_{cord}$ in people with MS ($r = 0.81$ (0.70–0.88), $p<0.0001$, Figure 3C) with a linear regression model slope of 0.88 and y-intercept 7.1 mm^2 ($r^2 = 0.73$). Bland-Altman analysis showed a

Figure 3. Correlation between C1 CSA from brain imaging and C2/3 CSA from cord imaging in healthy controls and people with multiple sclerosis (MS). A) Correlation between spinal cord cross-sectional areas (CSA) (mm^2) measured from healthy controls at C1 using brain imaging and at C2/3 using cord imaging. The r value was 0.84 with $p<0.0001$. A linear regression model was used to fit the data with r^2 value of 0.68, slope of 0.82, and y-intercept of 11 mm^2. The shaded area represents the 95% confidence interval ($n = 28$). (B) Bland-Altman plot for spinal cord CSA (mm^2) measured from healthy controls at C1 using brain images and at C2/3 using cord images. A bias of -1.9 mm^2 and 95% limits of agreement (shaded region) from -10 to 6.2 mm^2 were found. (C) Correlation between CSA (mm^2) measured from people with MS at C1 using brain imaging and at C2/3 using cord imaging. The r value was 0.81 with $p<0.0001$. A linear regression model was used to fit the data with r^2 value of 0.73, slope of 0.88, and y-intercept of 7.1 mm^2. The shaded area represents the 95% confidence interval ($n = 73$). (D) Bland-Altman plot for spinal cord CSA (mm^2) measured from people with MS at C1 using brain imaging and at C2/3 using cord imaging. A bias of -0.81 mm^2 and 95% limits of agreement (shaded region) from -10 to 8.6 mm^2 were found ($n = 73$).

bias of -0.81 mm^2, a 95% limit of agreement of -10 to 8.6 mm^2 and no significant non-zero slope ($p = 0.59$, Figure 3D).

Discussion

Strong relationships were found between all CSA measurements in both healthy controls and people with MS, obtained from spinal cord and brain images. Since C2/3 CSA is more commonly utilized in cord analysis and has been associated with disability as well as disease progression,[16–21] we first assessed whether high resolution spinal cord image CSA measurement at C1 (which can typically be assessed from brain images) yielded values consistent with those from C2/3. The strong linear correlation and even distribution of data points around the bias in the Bland-Altman analysis with non-significant slope support the use of C1

measurements as a suitable proxy for more commonly used C2/3 CSA in cord atrophy analysis. Although C2/3 is included in some brain MRI, it lies close to the edge of the FOV and can be affected by gradient non-linearities.[9] Furthermore, C2/3 is not as commonly or consistently covered in typical patient brain exams which could lead to biased results and reduced statistical significance.

Having established that C1 CSA can be used in place of C2/3 CSA, the consistency of C1 CSA measurements between dedicated spinal cord imaging and brain images was assessed. Once again, strong correlations and even distribution of data points around the bias with non-significant slope ($p = 0.16$) were demonstrated. The strong agreement between CSA measurements implies that dedicated cord imaging

may not be necessary for quantitative measurements of spinal cord atrophy, and that 3DT1 brain scans can provide the same information.

A small bias was observed when comparing the two values in healthy controls. A potential cause of this bias could be gradient non-linearities, however this is unlikely as the FOV of most brain images extends to C4 in the inferior caudal direction. Furthermore, the brain images have a sagittal readout with frequency encoding in the superior-inferior/foot-head direction, meaning that the superior-inferior FOV edges will be less affected by gradient non-linearities than in the right-left or anterior-posterior directions. A more likely reason could be the difference in contrast between T1- and T2*-weighted images causing different cord segmentation boundaries. The bias was not found in the larger group of people with MS and is inconsequential so long as measurements are taken from a consistent image contrast and that measurements from different image contrasts are not mixed.

Image resolution will also influence cord CSA measurement. Smaller voxels have improved accuracy due to less bias imposed by the method of thresholding the cord segmentation in the presence of partial volume effects, in voxels containing signal from both cord and cerebrospinal fluid. Reduced partial volume effects will be especially evident for smaller voxels in the superior-inferior direction, such as those acquired with a 3D isotropic acquisition, particularly in cases where the cord cannot be aligned perpendicularly to the superior-inferior imaging plane throughout the FOV.[22] Higher superior-inferior resolution will also improve the precision of cord CSA measurements, since CSA values will be averaged from more slices within each vertebral level and will therefore be less subject to the effects of outliers or the natural variation in size of the cervical cord along its length. Of course, the benefits of higher resolution acquisition come at the cost of longer acquisition times, making the images more prone to motion artefacts. Although determining the optimal sequence and resolution for CSA measurement is not trivial, high resolution isotropic 3D acquisitions are more easily accommodated by T1-weighted brain imaging sequences than by T2*-weighted cord imaging sequences (due to the much shorter TR and less difficult imaging environment), an additional benefit to calculating CSA from 3DT1 brain images.

Finally, we directly compared C1 CSA taken from brain images to C2/3 CSA measured from dedicated spinal cord imaging and found a strong relationship in both healthy controls ($r = 0.84$) and MS ($r = 0.81$). Taken all together, this study demonstrated that C1 CSA derived from brain images largely reflects C2/3 CSA measurements derived from cord images. This finding suggests that, when combined with the latest spinal cord image analysis tools, brain imaging can provide surrogate measures for cord atrophy. Furthermore, we observed minimal bias and a linear response reflecting changes in cord C2/3 CSA. This agrees with previous studies done by Liu et al. who showed that measurement at 2.5 cm below the pons in brain images is an appropriate surrogate for upper cord atrophy using semi- automated NeuroQLab software ($n = 97$), and Papinutto et al. who showed excellent C2-C3 area reliability when derived from brain scans using the semi-automated "cord finder option" in the JIM analysis software, which required multiple marker inputs ($n = 3$).[8,9] The current guidelines set by the ISCoS recommend the use of multi-gradient echo T2*-weighted scans centred at C2/3 for imaging and the use of JIM software or SCT for analysis of spinal cord atrophy.[10] Previous work in this area did not include a direct comparison to T2*-weighted cord imaging focused on validated C2/3 for measurement of CSA, or did not have a large sample size. Furthermore, our analysis used SCT, which is openly available and quickly becoming the standard for spinal cord image analysis. Our results are the first direct validation for the use of C1 CSA acquired from standard 3DT1 brain imaging as a surrogate for the C2/3 multi-gradient echo T2*-weighted cord-acquired CSA, as recommended by ISCoS, in the quantification spinal cord atrophy in people with MS.

Limitations

The specificity of CSA to pathological atrophy is one limitation of this metric. Processes such as inflammation[5] may confound results in people with MS. This may explain the slightly lower correlation coefficients between C1 and C2/3 measurements seen in people with MS. Furthermore, usage of C1 as surrogate for C2/3 will likely not suffice in studies investigating the structural-functional relationships specific to C2/3.

The images for this study were acquired from a single site which limits the generalizability of the study. However, use of only a single site avoids the confound of variability between scanners and scan parameters during initial assessment of the surrogate cord atrophy measure.

Structural variability is increased in the cervical region for people with MS which makes comparison between

individuals difficult.[18] Normalization to characteristics such as spinal cord length or participant height can be used to help remedy this issue, although some studies have shown that un-normalized values can provide increased sensitivity.[23] Alternatively, some studies advocate for newer slicewise normalization techniques.[24] Although our study circumvented the problem of inter-subject structural variability by comparing between acquisitions for the same individual, future studies investigating this issue in the context of CSA measurements derived from brain images would be valuable. Finally, as this study was cross-sectional, we cannot comment on how sensitive brain imaging-derived C1 CSA will be to changes in spinal cord imaging-derived C2/C3 CSA over time. Longitudinal acquisition is needed for comparison of changes in CSA over time between the different cord levels and image contrasts.

Significance and implications

The spinal cord plays an important role in MS disability and progression; spinal cord lesions are visible in over 80% of people with MS and correlate with clinical disability.[25] Spinal cord atrophy has become one of the strongest predictors of disability, showing greater association than the number or volume of lesions, especially for progressive phenotypes of MS.[1,26,27] CSA is also closely linked to measures of upper extremity function.[28,29] Even though cord atrophy can account for 77% of MS disability progression after 5 years, a surprisingly low number of progressive MS trials have used cord atrophy as an outcome measure.[3] In 2017, Moccia et al. highlighted the need for technical advancements to better facilitate robust cord atrophy measurements in clinical trials of MS, especially given the strong relationship between cord atrophy and disability.[2] The ability to derive a clinically relevant measure of cord atrophy from just a standard 3DT1 brain image can provide increased statistical power for progressive MS trials with just brain imaging, which would reduce the required sample size or length of the trial compared to using only standard brain imaging outcome measures. Alternatively, our approach could help reduce the cost of MRI booking time in cases where separate cord imaging is being acquired primarily for the purpose of measuring cord atrophy. In either case, this can make clinically feasible cord atrophy measurements accessible to help improve understanding of progression in MS and faster evaluate the efficacy of potential treatments.

Studies in MS brains have correlated brain size or "reserve" with resilience to MS pathology.[30] Specifically, larger brain and grey matter volume has been correlated with higher cognitive reserve and better cognitive function in MS.[31] Characterization of the natural variation in cord CSA can provide an opportunity to investigate the possibility of "spinal cord reserve" and to better distinguish pathological change from natural variation in MS.

Spinal cord images are prone to artefacts caused by cerebrospinal fluid flow, an inhomogeneous magnetic environment, small cord size, and cardiorespiratory motion.[6] Furthermore, MRI scanner coil changes are often required between collecting both brain and spinal cord images, increasing the scan time and patient discomfort. As a result, brain imaging is usually prioritized over spinal cord, meaning that cord images are often not acquired at all.[1]

In this study, imaging was performed using 8-channel and 6-channel receive coils designed specifically for brain and cervical cord imaging, respectively. Newer equivalent coils often have ~16–48 channels, leading to improved (reduced) g-factor and therefore higher signal-to-noise ratio, which will allow for improved image quality in the same acquisition time, or equivalent image quality in a reduced acquisition time. Some scanners are also equipped with a posterior spine coil built directly into the subject table, which improves cord-specific imaging, as well as large-FOV brain imaging where the posterior coil can contribute signal. The agreement demonstrated in this study between C1 CSA$_{brain}$ and C2/3 CSA$_{cord}$ should hold in the case of imaging using these more modern coils because the brain and cord imaging will each independently be improved. If anything, we expect the agreement to be improved by the use of brain imaging coils with more channels because they will provide a more comprehensive sensitivity profile across the imaging FOV. This is especially relevant to the edges of the FOV, such as the inferior caudal edge where the cord appears on 3DT1 brain images.

Removing the need for separate spinal cord scanning can drastically reduce the data acquisition time required for cord atrophy measures. This time-savings is compounded for most studies, where spinal cord imaging increases total exam time due to the data acquisition itself as well as the time necessary to change between head- and cord-specific imaging coils. One exception is for imaging with a combined head and neck coil, designed to perform both brain and cervical cord imaging using a single coil array, without necessitating a coil change. However, for these combined coils to fit the head and neck of most of the population, there generally must be fewer coil elements arranged further from the anatomies of interest, which poses a significant

disadvantage in terms of g-factor and signal-to-noise ratio compared to an anatomy-specific coil.[22] For example, a modern 16-channel head and neck coil will only have about half of those channels contributing to brain imaging, a substantial detriment compared to a 32-channel dedicated brain array. So, although a combined head and neck coil can perform brain and cord imaging without a coil change, it provides sub-optimal conditions compared to use of anatomy-specific coils and therefore still motivates the development of a brain imaging surrogate measure for cord atrophy. Reduced scan time has the benefit of improved patient comfort (especially important for imaging patient groups afflicted with physical disability or incontinence) and reduced susceptibility ot motion artefacts (especially important for cord imaging due to the presence of cardiac, respiratory, vascular, and vocal cord motion).[32]

Using C1 CSA from brain imaging as a proxy for C2/3 CSA from cord imaging also opens the possibility of performing retrospective spinal cord atrophy studies on cohorts and previously acquired data that did not include separate spinal cord imaging. Furthermore, our results highlight the value of including 3DT1 brain imaging as standard practice for clinical MRI exams in MS. Through the use of brain imaging derived C1 CSA, more research can now examine the connection between spinal cord atrophy and MS without being limited by availability and feasibility of spinal cord imaging.

Conclusion

C1 level spinal cord CSA calculated from brain scans is strongly correlated with C2/3 CSA calculated from separate, reference spinal cord imaging. This could prospectively and retrospectively provide studies with a convenient, clinically relevant measure related to spinal cord atrophy, without requiring separate dedicated cord imaging.

Declaration of conflicting interests

The author(s) declared no potential conflicts of interest with respect to the research, authorship, and/or publication of this article.

ORCID iDs

Kamyar Taheri https://orcid.org/0000-0002-6062-6983
Irene M Vavasour https://orcid.org/0000-0001-9286-0953
Shawna Abel https://orcid.org/0000-0001-8547-1415
Lisa Eunyoung Lee https://orcid.org/0000-0002-8334-3740
Nathalie Chantal Ackermans https://orcid.org/0000-0003-1469-259X
Robert Carruthers https://orcid.org/0000-0001-7085-1001
Adam Vladimir Dvorak https://orcid.org/0000-0001-6107-5610

References

1. Kearney H, Miller DH and Ciccarelli O. Spinal cord MRI in multiple sclerosis--diagnostic, prognostic and clinical value. *Nat Rev Neurol* 2015; 11: 327–338.
2. Moccia M, de Stefano N and Barkhof F. Imaging outcome measures for progressive multiple sclerosis trials. *Mult Scler* 2017; 23: 1614–1626.
3. Eden D, Gros C, Badji A, et al. Spatial distribution of multiple sclerosis lesions in the cervical spinal cord. *Brain* 2019; 142: 633–646.
4. Rocca MA, Valsasina P, Meani A, et al. Clinically relevant cranio-caudal patterns of cervical cord atrophy evolution in MS. *Neurology* 2019; 93 : e1852–e1866.
5. Klein JP, Arora A, Neema M, et al. A 3 T MR imaging investigation of the topography of whole spinal cord atrophy in multiple sclerosis. *Am J Neuroradiol* 2011; 32: 1138–1142.
6. Stroman PW, Wheeler-Kingshott C, Bacon M, et al. The current state-of-the-art of spinal cord imaging: methods. *Neuroimage* 2014; 84: 1070–1081.
7. Traboulsee A, Simon JH, Stone L, et al. Revised recommendations of the consortium of MS centers task force for a standardized MRI protocol and clinical guidelines for the diagnosis and follow-up of multiple sclerosis. *Am J Neuroradiol* 2016; 37: 394–401.

8. Liu Y, Lukas C, Steenwijk MD, et al. Multicenter validation of mean upper cervical cord area measurements from head 3D T1-weighted MR imaging in patients with multiple sclerosis. *Am J Neuroradiol* 2016; 37: 749–754.

9. Papinutto N, Bakshi R, Bischof A, et al. Gradient nonlinearity effects on upper cervical spinal cord area measurement from 3D T1 -weighted brain MRI acquisitions. *Magn Reson Med* 2018; 79: 1595–1601.

10. Seif M, Gandini Wheeler-Kingshott CA, Cohen-Adad J, et al. Guidelines for the conduct of clinical trials in spinal cord injury: neuroimaging biomarkers. *Spinal Cord* 2019; 57: 717–728.

11. Gros C, De Leener B, Badji A, et al. Automatic segmentation of the spinal cord and intramedullary multiple sclerosis lesions with convolutional neural networks. *Neuroimage* 2019; 184: 901–915.

12. De Leener B, Lévy S, Dupont SM, et al. SCT: spinal cord toolbox, an open-source software for processing spinal cord MRI data. *Neuroimage* 2017; 145: 24–43.

13. Thompson AJ, Banwell BL, Barkhof F, et al. Diagnosis of multiple sclerosis: 2017 revisions of the McDonald criteria. *Lancet Neurol* 2018; 17: 162–173.

14. Meyer-Moock S, Feng Y-S, Maeurer M, et al. Systematic literature review and validity evaluation of the expanded disability Status scale (EDSS) and the multiple sclerosis functional composite (MSFC) in patients with multiple sclerosis. *BMC Neurol* 2014; 14: 58.

15. De Leener B, Kadoury S and Cohen-Adad J. Robust, accurate and fast automatic segmentation of the spinal cord. *Neuroimage* 2014; 98: 528–536.

16. Lukas C, Knol DL, Sombekke MH, et al. Cervical spinal cord volume loss is related to clinical disability progression in multiple sclerosis. *J Neurol Neurosurg Psychiatry* 2015; 86: 410–418.

17. Brownlee W, Altmann D, Alves Da Mota P, et al. Association of asymptomatic spinal cord lesions and atrophy with disability 5 years after a clinically isolated syndrome. *Mult Scler J* 2017; 23: 665–674.

18. Biberacher V, Boucard CC, Schmidt P, et al. Atrophy and structural variability of the upper cervical cord in early multiple sclerosis. *Mult Scler J* 2015; 21: 875–884.

19. Kearney H, Rocca M, Valsasina P, et al. Magnetic resonance imaging correlates of physical disability in relapse onset multiple sclerosis of long disease duration. *Mult Scler J* 2014; 20: 72–80.

20. Furby J, Hayton T, Anderson V, et al. Magnetic resonance imaging measures of brain and spinal cord atrophy correlate with clinical impairment in secondary progressive multiple sclerosis. *Mult Scler* 2008; 14: 1068–1075.

21. Cawley N, Tur C, Prados F, et al. Spinal cord atrophy as a primary outcome measure in phase II trials of progressive multiple sclerosis. *Multiple Sclerosis Journal* 2018; 24: 932–941.

22. Cohen-Adad J and Wheeler-Kingshott C. *Quantitative MRI of the spinal cord*. Cambridge, Massachusetts, USA: Academic Press, 2014.

23. Zivadinov R, Banas AC, Yella V, et al. Comparison of three different methods for measurement of cervical cord atrophy in multiple sclerosis. *Am J Neuroradiol* 2008; 29: 319–325.

24. Healy BC, Arora A, Hayden DL, et al. Approaches to normalization of spinal cord volume: application to multiple sclerosis. *J Neuroimaging* 2012; 22: e12–e19.

25. Bot JCJ, Barkhof F, Polman CH, et al. Spinal cord abnormalities in recently diagnosed MS patients: added value of spinal MRI examination. *Neurology* 2004; 62: 226–233.

26. Valsasina P, Aboulwafa M, Preziosa P, et al. Cervical cord T1-weighted hypointense lesions at MR imaging in multiple sclerosis: relationship to cord atrophy and disability. *Radiology* 2018; 288: 234–244.

27. Liu Z, Yaldizli Ö, Pardini M, et al. Cervical cord area measurement using volumetric brain magnetic resonance imaging in multiple sclerosis. *Mult Scler Relat Disord* 2015; 4: 52–57.

28. Aymerich FX, Auger C, Alonso J, et al. Cervical cord atrophy and long-term disease progression in patients with primary-progressive multiple sclerosis. *Am J Neuroradiol* 2018; 39: 399–404.

29. Zurawski J, Glanz BI, Healy BC, et al. The impact of cervical spinal cord atrophy on quality of life in multiple sclerosis. *J Neurol Sci* 2019; 403: 38–43.

30. Sumowski JF, Rocca MA, Leavitt VM, et al. Brain reserve and cognitive reserve in multiple sclerosis: what you've got and how you use it. *Neurology* 2013; 81: 604–604.

31. Fenu G, Lorefice L, Arru M, et al. Cognition in multiple sclerosis: between cognitive reserve and brain volume. *J Neurol Sci* 2018; 386: 19–22.

32. Gückel B, Gatidis S, Enck P, et al. Patient comfort during positron emission tomography/magnetic resonance and positron emission tomography/computed tomography examinations. *Invest Radiol* 2015; 50: 726–732.